Spin-resolved photoemission from (111) surfaces of Pd, Ir and Pt by circularly polarised light: theory and comparison with experiment

1989 J. Phys.: Condens. Matter 1 6469

(http://iopscience.iop.org/0953-8984/1/36/015)

J. Phys.: Condens. Matter 1 (1989) 6469–6482. Printed in the UK

Spin-resolved photoemission from (111) surfaces of Pd, Ir and Pt by circularly polarised light: theory and comparison with experiment

E Tamura†, W Piepke and R Feder
Theoretische Festkörperphysik, Universität-Duisburg-GH, D-4100 Duisburg, West Germany

Received 19 September 1988, in final form 27 February 1989

Abstract. A fully relativistic one-step theory of photoemission has been applied to calculate spin-resolved normal-emission spectra induced by circularly polarised photons between 6 and 25 eV from the unreconstructed (111) surfaces of Pd, Ir and Pt. Consistent with the simultaneously calculated bulk band structures, individual spectral features are identified as bulk interband transitions and one-dimensional density of states transitions between initial and final states of specific double-group symmetry types. Theoretical peaks have experimental counterparts, with some deviations (up to 0.3 eV) in energy, but the observed spectra exhibit in addition 'ghost peaks' reflecting dominant peaks in the opposite-spin spectra, which—beyond experimental artifact—indicates some spin-flip process. Relative peak heights are in reasonable agreement except for an observed enhancement for photon energies such that the final states are associated with a flat f-like band.

1. Introduction

Analysis of the electron spin polarisation in angle-resolved photoemission spectroscopy provides information both on the electronic structure of the solid-surface system under study and on the emission mechanism, which cannot be obtained from intensity spectra (for reviews and references, cf Feder 1985, Kirschner 1985, Schönhense 1986, Heinzmann 1987). For non-magnetic systems, this is a consequence of spin–orbit coupling in the photoelectron (final) state or hole (initial) state. To extract the full wealth of physical information contained in experimental data, comparison is needed with corresponding spectra calculated by a quantitatively adequate theory. To this end, fully relativistic one-step model formalisms of photoemission from semi-infinite crystalline solids have been developed (Ackermann and Feder 1985a, b; Ginatempo *et al* 1985, Braun *et al* 1985), but their numerical applications are still quite scarce. For normal emission from Pt (111), spin polarisation due to circularly polarised light was calculated (Ackermann and Feder 1985b, Ginatempo *et al* 1985) and compared with experiment (Oepen *et al* 1985) for one photon energy, and a new spin polarisation effect produced by linearly polarised light was theoretically predicted by Tamura, Piepke and Feder (1987) in good agreement with subsequent experimental findings by Schmiedeskamp, Vogt and Heinzmann (1988).

† Present address: Institut für Festkörperforschung, KFA Jülich, 5170 Jülich, West Germany.

0953-8984/89/366469 + 14 $02.50

As extensive spin-resolved experimental data have been obtained by circularly polarised synchrotron radiation for normal emission from Pt(111) (Eyers *et al* 1984, Oepen *et al* 1985), Ir (111) (Müller *et al* 1987) and Pd(111) (Schmiedeskamp *et al* 1988), theoretical studies for these unreconstructed FCC(111) surfaces seem particularly worthwhile. In this paper, we present results obtained by applying the relativistic one-step-model theory of Ackermann and Feder (1985a, b) and compare them with the corresponding data. The quantitative agreement reached demonstrates the adequacy of this type of theory and allows a detailed physical interpretation of the experimental spectra.

In § 2, we recall some key features of the formalism and describe the specific model assumptions underlying the numerical calculations. In § 3, bulk band structures and calculated spin-resolved spectra for the (111) surfaces of Pd, Ir and Pt are presented and used for analysing the experimental data.

2. Theory

The theoretical formalism, which we employ, has been presented earlier (Ackermann and Feder 1985a, b). It may therefore suffice to recall some of its key features. The interaction of the photoelectron and of the 'hole' with a crystal, which is infinite in two dimensions (parallel to the surface) and finite or semi-infinite in the third, is described in an effective Dirac Hamiltonian by a quasiparticle self-energy term, which for non-magnetic systems is an energy-dependent local complex scalar potential $V(E, \boldsymbol{r})$. Its imaginary part corresponds to the inverse lifetime of the electron or hole. Thermal lattice vibrations are presently not included. The photoelectron (final) state is a spin-polarised LEED state going backwards in time. The hole can be described (a) by a Green function or (b) by a stationary half-space initial state wave function, which is obtained by matching Bloch waves incident on the surface from inside the crystal to reflected ones. In approach (b) the elastic photocurrent spin density matrix $\rho(E, \boldsymbol{k}_\parallel)$ is given by golden-rule-type dipole matrix elements between final and initial states. In contrast to the Green function approach (a), the initial state lifetime is not included *a priori* but taken into account by convoluting $\rho(E, \boldsymbol{k}_\parallel)$ with a Lorentzian. We have chosen approach (b) in this study, since firstly it is computationally simpler and secondly the contributions to $\rho(E, \boldsymbol{k}_\parallel)$ from individual initial states are obtained separately, which facilitates the physical interpretation.

The observable quantities, intensity I and spin polarisation vector $\boldsymbol{P}$ of the photocurrent, are obtained from the spin density matrix ρ as $I = tr[\rho]$ and $\boldsymbol{P} = \mathrm{tr}[\boldsymbol{\sigma}\rho]/\mathrm{tr}[\rho]$, where $\boldsymbol{\sigma}$ comprises the Pauli spin matrices. Some general properties of $\boldsymbol{P}$ can be obtained, without numerical calculations, by symmetry considerations in the one-step model. For circularly polarised radiation incident and electrons emitted perpendicular to a (centrosymmetric crystal) surface, with the surface normal parallel to an n-fold (with $n \geqslant 2$) rotation axis of the crystal, rotation symmetry of the entire set-up dictates that $\boldsymbol{P}$ is normal to the surface. If there is, in addition, a mirror plane perpendicular to the surface, reversal of the photon helicity and of $\boldsymbol{P}$ by the mirror operation entails a sign change of $\boldsymbol{P}$ upon reversal of the photon helicity. (For linearly polarised light and a 3-fold axis, the rotation symmetry of the set-up is broken and $\boldsymbol{P}$ parallel to the surface becomes possible (Tamura *et al* 1987 and Schmiedeskamp *et al* 1988)).

The sign and the magnitude of P (normal to the surface) for electrons originating from a given initial state can be obtained by group theoretical arguments, involving the

double group of C_{3v} for the (111) faces under consideration (cf reviews by Wöhlecke and Borstel 1984 and Feder 1985, and references therein). The final state, which consists of plane waves on the vacuum side, has double group symmetry Λ_6, i.e. is a linear combination of basis functions characterised by Λ_6^1, Λ_6^2 and Λ_6^3. In this notation, the subscript indicates the extra irreducible representation of the double group and the superscript characterises the spatial part of the (spinor) function by the label of the single group under which it transforms. (For details on this notation, which has become standard in relativistic photoemission work, cf. Wöhlecke and Borstel 1984 Section 4, Feder 1985 p 209f, and references therein). For transitions from initial states of Λ_{4+5}^3 symmetry to final states Λ_6^1 and Λ_6^2 one has $P = +1$, and to final states Λ_6^3 $P = -1$ (with light of positive helicity incident on the surface and $P = +/-$ defined as parallel or antiparallel to the momentum of the outgoing photoelectron). Consequently, for 'hybridised' final states, containing e.g. both a Λ_6^1 and a Λ_6^3 part, $|P| < 1$ (i.e. less than 100% spin polarisation). It thus appears that, for a given initial state, sign and magnitude of P depend on details of the final state. To make contact with experimental reality it is, however, important to note that the final state is a time-reversed LEED state (cf e.g. Feibelman and Eastman 1974) and that only its outgoing part, a plane wave of Λ_6^1 symmetry, reaches the detector. Therefore one observes, for Λ_{4+5} initial states, always $P = +1$. Similarly, for Λ_6 initial states one always finds $P = -1$. It is therefore useful to define partial intensities

$$I_\sigma = I(1 + \sigma P)/2 \qquad \text{with} \qquad \sigma = +/- \tag{1}$$

which originate from Λ_{4+5} and Λ_6 initial states, respectively.

We now specify the model assumptions underlying our calculations for the (111) surfaces of Pd, Ir and Pt. Since these surfaces are known to be unreconstructed with practically no displacement of the topmost layer, the geometry is that of a truncated bulk crystal. The effective potential is assumed to have the muffin tin shape. Its (spherically symmetric) ion-core scattering part is taken from recent self-consistent ground state calculations by the LMTO-ASA method using the local exchange-correlation approximation by Barth and Hedin (1972) (Christensen 1987). The real part of the uniform inner potential for the initial states is taken as $E_F + \Phi$ (E_F denoting the Fermi energy and Φ the work function), giving 13.9, 17.0 and 15.0 eV for Pd, Ir and Pt, respectively. For the final states it is assumed as reduced by 1 eV, an average value in the appropriate energy range guided by low-energy-electron diffraction and target current analyses for W(001) and Fe(001) (Baribeau *et al* 1985, Tamura *et al* 1985, and references therein), and also suggested by secondary electron-emission and photoemission data for Ir (Müller *et al* 1987, and references therein) and Pd (Schmiedeskamp *et al* 1988). The hole lifetime is described by an imaginary self-energy part, which rises linearly (cf. Eberhardt and Plummer 1980) as 0.1 $(E - E_F)$ eV with the distance from E_F. We also employed a quadratic form (cf. Treglia *et al* 1982) $(E - E_F)^2/[(E - E_F)^2 + E_0]^2$ eV with the parameter E_0 chosen as 4 eV (e.g. 0.2 and 0.5 eV for $E - E_F = -2$ and -4 eV). For the final state lifetime we adopted an imaginary potential form (McRae and Caldwell (1976)) $a(E - E_F)^b$ with $a = 0.025$ and $b = 1.25$. The surface potential barrier is approximated by a refracting step, which is reflecting for the initial state and non-reflecting for the final state. The latter choice is guided by the LEED experience that a reflecting step barrier strongly exaggerates the reflectivity in the very low energy regime (compared to a realistic continuous barrier).

3. Numerical results and comparison with experiment

We now present a selection of normal-emission spin-resolved photoelectron spectra $I_+(E)$ and $I_-(E)$ calculated at various photon energies for the (111) faces of Pd, Ir and Pt. Individual spectral features are interpreted in terms of direct transitions between bulk states along $\Gamma(\Lambda)$L as obtained from our effective potential, taking only the real part for the initial states and the real and imaginary part for the upper states.

In comparing the calculated spectra with their experimental counterparts, the following points have to be borne in mind: (a) The experimental spectra $I_0(E)$ and $P_0(E)$ contain inelastic contributions. Assuming them as unpolarised (because of integrations over E and $k_\parallel$) and denoting them as $I_b(E)$, background-corrected partial intensities $I_\pm$ are obtained by equation (1) using

$$I(E) = I_0(E) - I_b(E) \qquad \text{and} \qquad P(E) = P_0(E)I_0(E)/I(E). \tag{2}$$

(b) The degree of circular polarisation of the synchrotron radiation is only about 90%. Consequently, the experimental partial intensity spectra contain a 10% fraction originating from 'opposite symmetry' initial states. (c) The experimental resolution was about 0.25 eV in energy and $\pm 3°$ in the polar emission angle.

3.1. Pd(111)

The calculated spectra for photon energies 16, 21 and 23 eV (figure 1) exhibit two I_+ peaks, labelled A and D, and two I_- peaks, labelled B and C. To explain their physical origin, we consider the lower and upper bulk band structures along $\Gamma(\Lambda)$L (figure 2). The hole state bands (below E_F)—calculated using the real potential described above—from which transitions are allowed by relativistic dipole selection rules, belong to double group symmetry Λ_6 and Λ_{4+5}. Since, however, only states with dominant Λ^3 spatial part contribute appreciably to the photocurrent, we have to focus on the two pairs of flat bands between E_F and -1 eV, and -2 and -3 eV, respectively. We recall that the splitting between the bands in each pair is a consequence of spin–orbit coupling. The final state bands of Λ_6^1 symmetry type—as obtained from the real part of the potential—are seen (in figure 2) to consist of a free-electron-like band starting at 8 eV and a flat f-like band between 16.5 and 18 eV, with a hybridisation gap around 18.5 eV. Inclusion of an imaginary potential part changes these bands into those labelled 1 to 3 and adds non-zero imaginary parts to the wave-vector component k_z. We notice that $\mathrm{Im}k_z$ for the free-electron-like band 1 is far smaller than $\mathrm{Im}k_z$ for band 2 and 3. (For a detailed discussion of the influence of an imaginary potential part we refer to Hora and Scheffler (1984)). This slower decay of band 1 states and their stronger coupling to the plane wave in vacuum suggests them to provide the dominant final states.

As is explicitly shown by the vertical lines for photon energy $\hbar\omega = 16$ eV in figure 2, the origin of the calculated photoemission peaks A to D (in figure 1) is identified as bulk inter-band transitions, with I_+(A, D) and I_-(B, C) associated with initial states of symmetry Λ_{4+5}^3 and Λ_6^3, respectively. Variation of the photon energy between 6 and 23 eV changes the $\mathrm{Re}k_z$, at which the transition takes place, between L and Γ, and consequently permits a 'mapping' of the initial state bands. The small peaks around 0.2 in I_+ and 0.4 eV in I_- for $\hbar\omega = 16$ eV cannot be interpreted as direct transitions near 0.9ΓL, but rather as 'density-of-states' transitions into a strongly evanescent gap state, with $\mathrm{Im}k_z$ about 0.3. For photon energies around 6 eV, peaks A and B are seen from figure 2 to arise from direct transitions into the complex-potential band 1 near L.

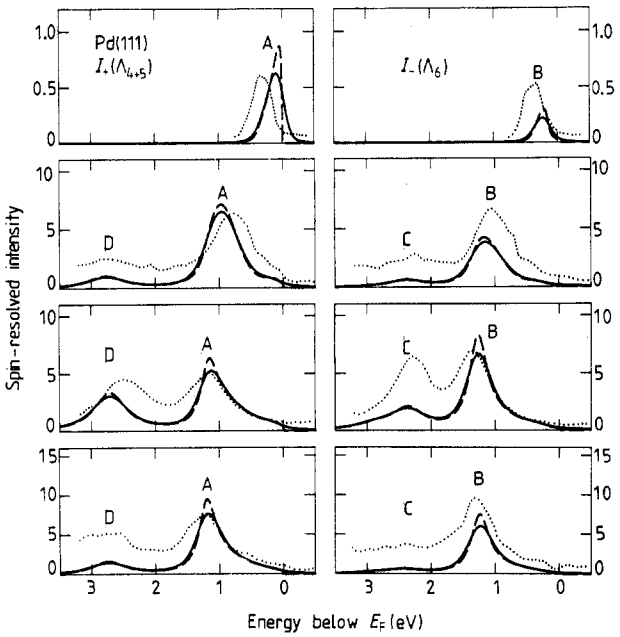

Figure 1. Normal photoemission from Pd(111) by normally incident circularly polarised radiation. The left (right) column shows partial intensity spectra $I_+(I_-)$ (cf eq. (1)) arising from $\Lambda_{4+5}(\Lambda_6)$ initial states. The theoretical spectra were obtained with a linearly rising hole damping (———) and an additional broadening by a Gaussian of 0.25 eV FWHM (———). The experimental spectra are due to Schmiedeskamp *et al* 1988. The photon energies (from top to bottom) are: 6, 16, 21 and 23 eV. The 0 on the abscissa corresponds to the Fermi level. The intensity values refer to our calculation (multiplied by a constant factor). (Note the reduction of scales with increasing photon energy). The experimental data are scaled such that at each photon energy the height of the leading I^+ peak (A) matches its theoretical counterpart.

Comparing our results with the experimental spin-resolved spectra of Schmiedeskamp *et al* (1988) (cf. figure 1), we find that the dominant features A to D agree with regard to existence and approximate position (energy). In particular, the spin–orbit splitting of the two occupied Λ^3 pairs around 0.5ΓL, given by the distances between A and B and between C and D in the 16 eV spectra, is seen to agree (about 0.25 eV for the upper and about 0.4 eV for the lower pair). Our calculations thus confirm the physical interpretation of the observed features given by Schmiedeskamp *et al* (1988) in terms of bulk interband transitions originating from initial states of symmetries Λ^3_{4+5} and Λ^3_6. This also holds at photon energy 6 eV, for which the final state lies in a gap of the real bulk band structure and on a band with a complex k_z if final-state life-time is taken into account.

The discrepancies up to about 0.2 eV in the positions of the peaks could not be removed by calculations, in which the self-energy of the upper state was varied within physically reasonable limits. We therefore interpret them as differences between quasiparticle energies (as observed by photoemission) and ground state one-electron energy bands. To what extent these differences are due to approximations made in calculating the latter (in particular the local density approximation) or to self-energy corrections, is still an outstanding theoretical problem.

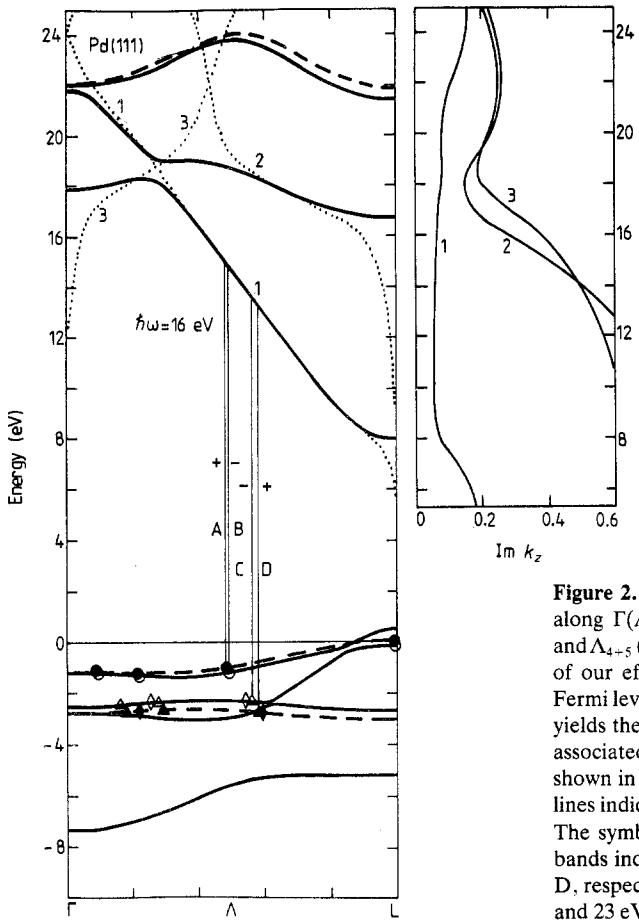

Figure 2. Relativistic bulk band structure of Pd along $\Gamma(\Lambda)L$ with symmetry types Λ_6 (———) and Λ_{4+5} (— — —), as obtained from the real part of our effective potential. The energy 0 is the Fermi level. Inclusion of the imaginary part of V_2 yields the (· · · ·) bands labelled 1, 2, 3, and the associated imaginary parts of the wave-vector shown in the right-hand-side panel. The vertical lines indicate transitions at photon energy 16 eV. The symbols ●, ○, ▲ and △ on the occupied bands indicate the origins of peaks A, B, C and D, respectively, for the photon energies 6, 16, 21 and 23 eV. ◆ and ◇ indicate initial states, from which, at $\hbar\omega = 21$ eV, transitions may occur into the flat f-like band around 18 eV.

With regard to peak heights we firstly note that at $\hbar\omega = 21$ eV the calculated intensities D and C are lower (relative to A and B) by a factor between 2 and 3 than the experimental ones (after subtraction of an inelastic background). This enhancement of the latter was measured in detail (Schmiedeskamp *et al* 1988) as a function of the photon energy and found to be maximal for final state energy 18.8 eV, i.e. in the real band structure (cf figure 2) in the hybridisation gap produced by the free-electron band and the flat f-like band. In terms of the complex band structure, three direct transitions are seen to be allowed instead of usually one. Our photoemission calculations also produce such enhancement (as illustrated in figure 1 by the heights of C and D at 16, 21 and 23 eV), but by a factor of at least 2 smaller than experiment. The spin-average of our 21 eV spectra agrees well with non-relativistic one-step model results (Hora and Scheffler 1984), with the latter also failing to reproduce the observed CD enhancement. It thus appears that present-day one-step formalisms do not take account of the physical mechanism, which produces this 'resonance'.

Further, in most of our calculated spectra peak A is substantially stronger relative to its opposite-spin partner B than in the experimental data. This finding is, via equation

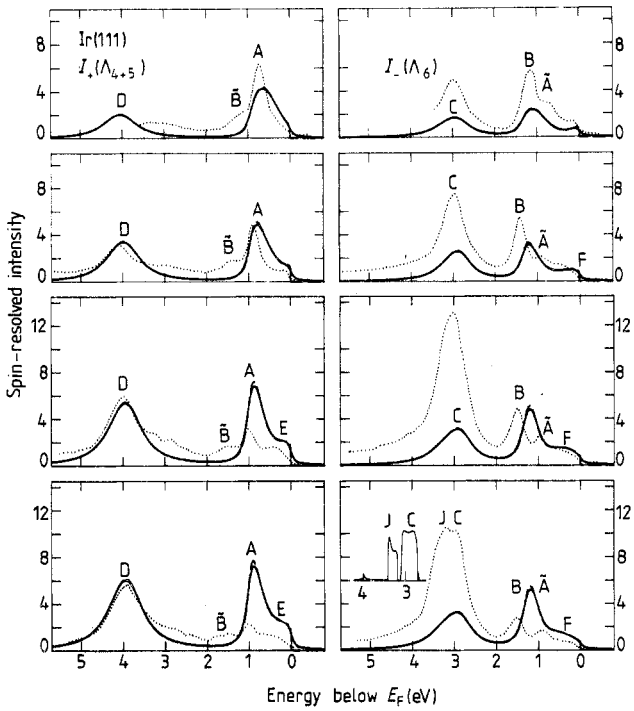

Figure 3. Normal photoemission from Ir(111). Analogous to figure 1, but with experimental spectra (· · · ·) from Müller *et al* (1987)—rescaled such that at $\hbar\omega = 16$ eV the height of peak A matches theory. The Gaussian width (used in ———) is 0.15 eV. The inset in the 17.6 eV Λ_6 panel shows J and C as obtained in a calculation with hole life-time potential part $V_{il} = 0$. The photon energies (from top to bottom) are: 15, 16, 17.2 and 17.6 eV.

(1), related to an excess of the calculated spin polarisation at the energy of A over the experimental one. Some hint for an explanation is given by the appearance in experimental I_- spectra (e.g. at 6, 16 and 23 eV in figure 1) of a shoulder on the right-hand-side of B at the energy of A. It looks as if weight was transferred from A to this opposite-spin 'ghost peak', possibly by spin-flip scattering in the final state. An explanation by additional phonon-induced transitions appears less likely firstly since the phenomenon occurs for a wide range of initial state energies and secondly, since the data were taken at 60 K corresponding to 22% of the Debye temperature.

3.2. Ir(111)

The presentation and discussion of spin-resolved photoemission results from Ir(111) is analogous to the above for Pd(111) and therefore very concise except with regard to some new features and aspects. Representative spectra are shown in figure 3. The theoretical spectra exhibit against four main peaks (labelled A to D) and two smaller ones (E and F), which can be understood as due to bulk interband transitions originating at the points marked in the occupied part of the band structure (shown in figure 4). For $\hbar\omega = 16$ eV we have made this more explicit by adding vertical transition lines in figure 4. We note the agreement with the bulk interband transition interpretation given by Noffke and Fritsche (1982). The 16 eV transition near Γ into the f-like band is allowed,

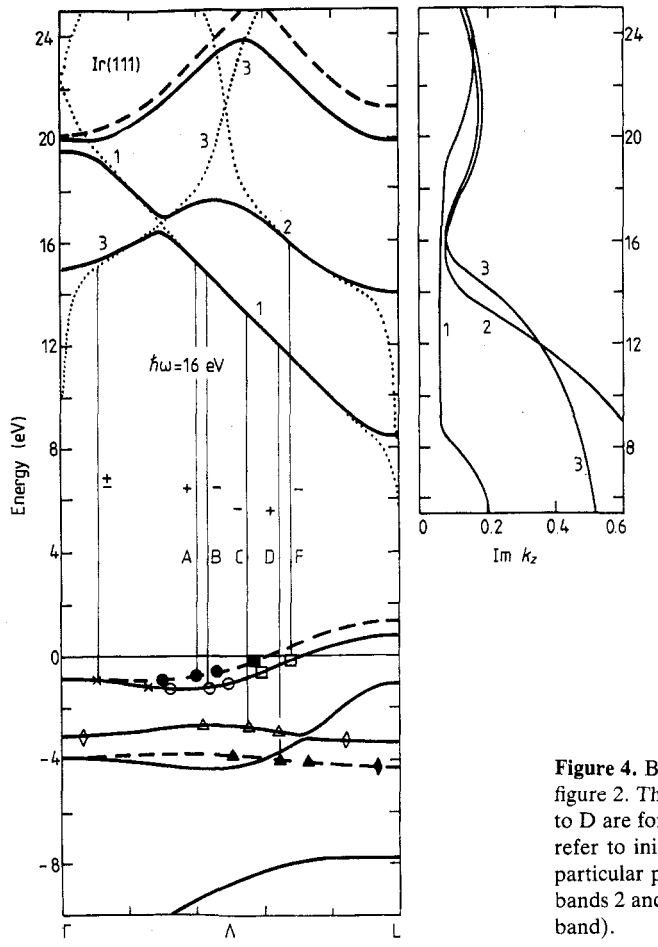

Figure 4. Bulk bands of Ir along Λ analogous to figure 2. The symbols indicating the origins of A to D are for $\hbar\omega$ = 15, 16 and 17.6 eV. ◆ and ◇ refer to initial states for 17.6 eV transitions (in particular peak J) into the unoccupied complex bands 2 and 3 (associated with the real flat f-like band).

but does not produce a photoemission peak. At $\hbar\omega = 17.6$ eV, peak C has a shoulder, which by a calculation neglecting hole life-time is revealed (see inset in figure 3) as an additional transition (peak J) from the lower Λ_6^3 band near L into the flat f-like final state band. The spin–orbit splitting of the two occupied Λ^3 bands is, due to the larger atomic number of Ir ($Z = 77$), larger than for Pd ($Z = 46$): e.g. halfway along ΓL 0.43 eV and 1.15 eV for the upper and lower pair, respectively.

Comparison with the experimental spectra of Müller *et al* (1988) (cf. figure 3) shows agreement in existence and energy position of features A to F. The slight shift of the experimental B for $\hbar\omega \geqslant 16$ eV indicates that between 0.2 and 0.5 ΓL the upper occupied quasi-particle Λ_6^3 band is lowered by about 0.2 eV relative to the local-density-approximation ground state band shown in figure 4.

In relative intensities, we find—as above for Pd(111)—that our theory fails to produce the 'resonant enhancement' of peaks C and D relative to B and A, respectively, which is observed when final states near the flat f-like band become accessible. This discrepancy is linked with the unusual finding that at the energy of C the measured spin polarisation (−80%) substantially exceeds the calculated value (−60%). A further discrepancy shows up in the height of A relative to B. As already found above the Pd(111), the theoretical values strongly exceed the experimental ones.

The experimental spectra again—and more distinctly than for Pd(111) with its smaller spin-orbit splitting—exhibit opposite-spin ghost peaks, labelled $\tilde{A}$ and $\tilde{B}$ in figure 3, at the energies of A and B, respectively. According to Schmiedeskamp *et al* (1988), these ghosts are not experimental artifacts (as could for example be produced by a systematically too low spin polarisation measurement), but physically significant. They cannot be caused by some Λ_6^3-symmetry admixture to the mainly Λ_6^1 final state: firstly on the grounds of our general argument given above (prior to equation (1)) and secondly because our calculations include such admixture but do not produce any ghost peak. Nor are they due to off-normal contributions in the experimental $\pm 3°$ acceptance cone, since spectra calculated for $\theta = 3°$ and selected azimuths agree with the $\theta = 0$ spectra within less than 2%. In search for an explanation we note that in the experimental spectra the height of A is less or equal to that of B, while $\tilde{A}$ is larger than $\tilde{B}$. Spin-flipping the ghosts back into their partners adds more weight to A than to B, and thereby somewhat reduces the A/B height ratio discrepancy with theory.

3.3. Pt (111)

Since the atomic number and the number of d electrons per atom increase by only one from Ir to Pt ($Z = 78$), bulk band structure and photoemission spectra are rather similar, with the upper occupied Λ^3 pair by about 1 eV lower relative to E_F. The calculated spin-resolved spectra, a selection of which is shown in figure 5, again consist mainly of the four peaks A to D produced by bulk interband transitions into the free-electron-like band 1 (see figure 6, with vertical transition lines drawn for $\hbar\omega = 17$ eV). The small features E and F in the 17 eV spectra are due to transitions into the f-like band 2. The weak shoulder at -0.5 eV in the 19 eV and 21 eV I_- spectra arises from the high density of Λ_6^3 states near L by excitation into strongly evanescent final states. A further feature (labelled G) emerges in the $I_-(\Lambda_6)$ spectra for $\hbar\omega = 19$ eV near -4.2 eV and grows with increasing photon energy. It can be interpreted by transitions from Λ_6 initial states (band around -4.2 eV) into band 3 states. The increase with phonon energy is a consequence of an increasing Λ_6^3 admixture to the mainly Λ_6^1 initial state as k_z moves away from Γ. A corresponding transition from the lower Λ_{4+5} band into band 3 is masked by peak D. The 17 eV transition from the upper Λ^3 pair near Γ (shown in figure 6) is allowed, but does not produce a peak.

In addition to the intensity spectra, we display (in the third column of figure 5) spin polarisation spectra obtained via equation (1) without (dash-dotted curves) and with (dashed and full curves) a linearly rising unpolarised background intensity (shown in the I_+ and I_- spectra). Although strictly speaking redundant, the P spectra offer a complementary view and are useful for extracting information from the experimental data. The sign of P at the energies of the main intensity peaks is seen to be in accordance with group theoretical prediction: positive (negative) for initial states of symmetry Λ_{4+5} (Λ_6). Its magnitude is reduced from unity (100%) by life-time broadening, with calculated maximal values of 80% for peaks A and D, which do not have 'stronger neighbours'. (For $\hbar\omega = 25$ eV, the opposite-spin G coincides in energy with D, reducing P to about 10%). Addition of an inelastic background further reduces P: e.g. for peak D from 80% to about 40%. At small binding energies, where hole damping and background are small, the 0.3 eV Gaussian broadening corresponding to experimental energy resolution is seen to lead to a further decrease of P.

The level of agreement between theoretical and experimental partial intensity spectra (see figure 5) is similar to that found above for Pd and Ir. In particular, we notice

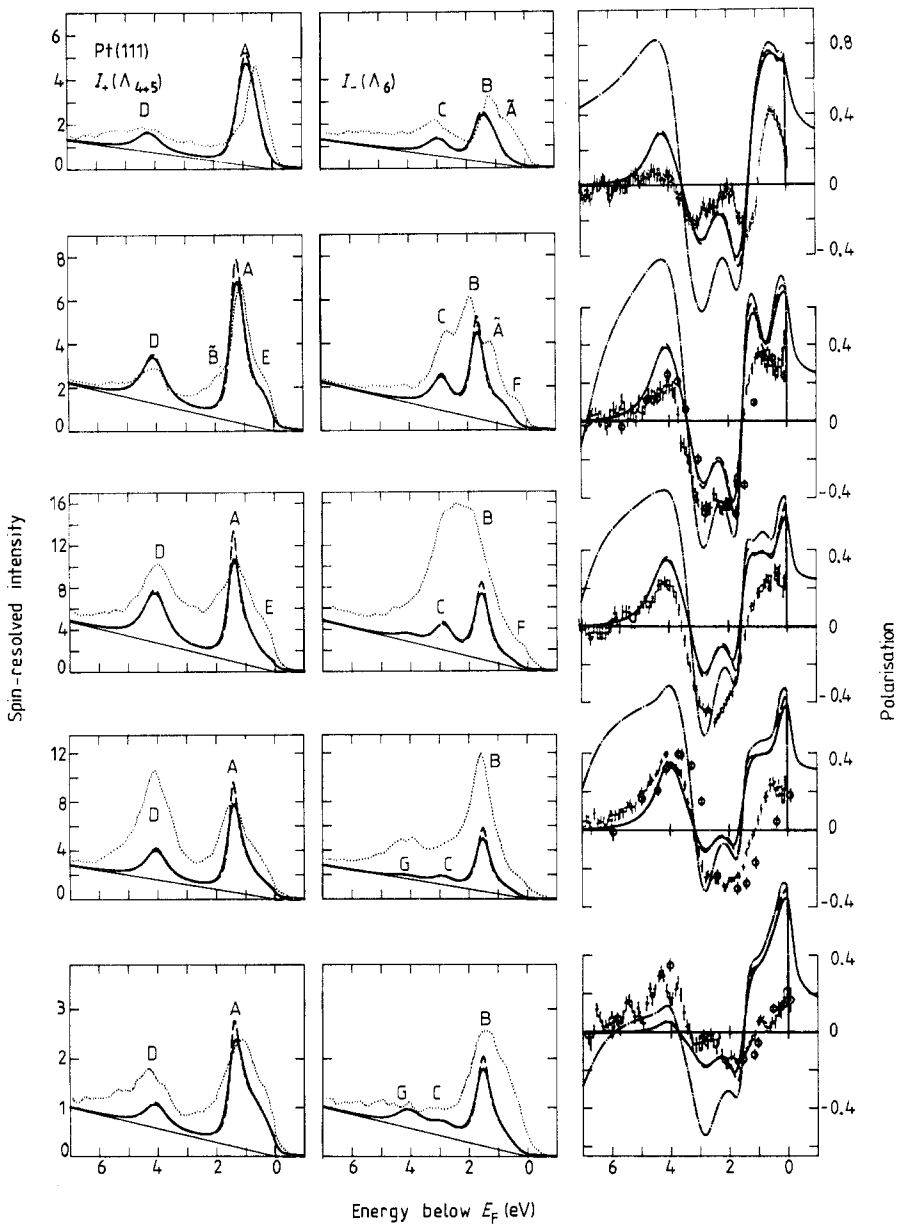

Figure 5. Normal photoemission from Pt(111). Partial intensity spectra analogous to figure 1, with experiment (· · · ·) from Garbe and Kirschner (1988). The Gaussian width (used in ———) is 0.30 eV. The third column gives the corresponding spin polarisation spectra: Theory without (— · —) and with linearly rising unpolarised inelastic background without (— — —) and with (———) Gaussian broadening, experiment by Garbe and Kirschner (1988) (●) and by Eyers *et al* (1984) (○). Photon energies (from top to bottom): 13, 17, 19, 21 and 25 eV.

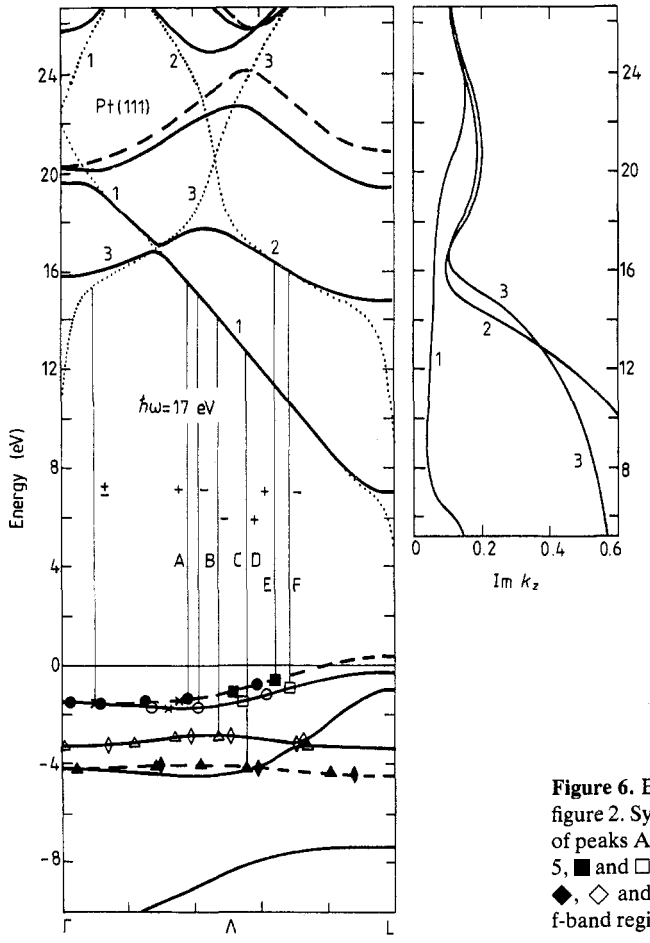

Figure 6. Bulk bands of Pt along Λ analogous to figure 2. Symbols ●, ○, ▲ and △ indicate origins of peaks A to D for the photon energies in figure 5, ■ and □ peaks E and F for $\hbar\omega = 17$ and 19 eV, ◆, ◇ and x 'resonant' transitions into the flat f-band region (around final state energy 16 eV).

again in the experimental data a 'resonant enhancement' of C and D (for 19 and 21 eV) (which was also found in spin-averaged measurements by Wern *et al* (1985)) and the opposite-spin ghost peaks $\bar{A}$ and $\bar{B}$. The latter, by virtue of equation (1), are associated with a reduction of the observed spin polarisation P around the respective energies, can be seen in the right-hand column of figure 5. As factors contributing to ghosts and P reduction we can identify: (a) the incomplete (about 90%) circular polarisation of the radiation used, and (b) phonon-induced indirect transitions (involving states $k_\parallel \neq 0$), since the data reproduced in figure 5 were obtained at room temperature and cooling to 40 K was found (cf. Eyers *et al* 1985) to increase P at the energies of peaks A and B by about 10 to 15%. It appears, however, that this still leaves a residual discrepancy. Intensity resonances for peaks C and D are reflected in the polarisation spectra and can in particular lead to observed values much larger than the calculated ones (e.g. for peak C at 19 and 21 eV). Further away from E_F, where the background is larger, we also have to bear in mind that P as calculated with background depends on the relative magnitude of the assumed background, i.e. in figure 5 on the scaling of the experimental data to match a selected peak (A in figure 5). For $\hbar\omega = 25$ eV, peak intensities are lower by a factor between 2 to 5 compared to the other photon energies. This is readily understood,

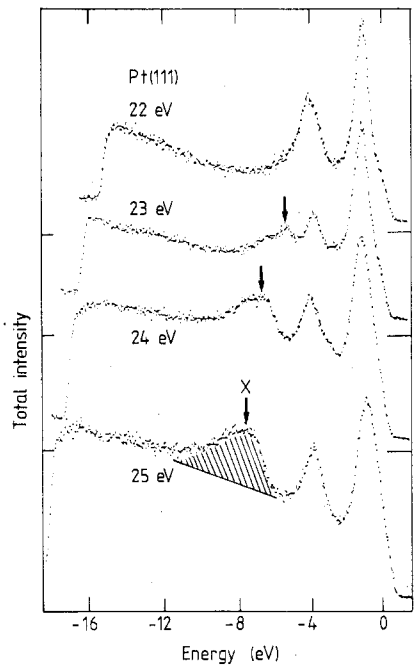

Figure 7. Experimental total intensity spectra for normal emission from Pt(111) at photon energies between 22 and 25 eV (from Eyers *et al* 1984 and Eyers 1984). Downward arrows indicate peaks due to secondary electron emission.

since the upper state energies (cf. figure 6) are in a gap between the mainly Λ_6^1 bands, and the flat Λ_6^3-like band between 20 and 22 eV couples only very weakly to the vacuum.

For photon energies between 22 and 25 eV, total intensity spectra measured by Eyers *et al* (1984) (see figure 7)—and likewise by Garbe and Kirschner (1988)—exhibit a broad asymmetric peak at binding energies below 4.5 eV i.e. below the ΓL d-bands. Most pronounced for $\hbar\omega = 25$ eV, it is seen to move towards smaller binding energy with decreasing $\hbar\omega$ such that the final state energy remains constant. As can be seen from our band structure (figure 6), the energy range of the peak falls in the range of the flat f-like band with its high density of states. This suggests an interpretation in terms of secondary electron emission. Closer inspection of the spectra (figure 7) indicates that the feature actually consists of two peaks with maxima corresponding to final state energies of about 16.5 and 17.5 eV, i.e. moved slightly away from the critical points into the interior of the band. As has been demonstrated earlier (Tamura and Feder 1986, Tamura *et al* 1985 and references therein), such energy position is charcteristic for fine structure features in secondary electron emission. For $\hbar\omega = 22$ eV, it appears to merge into the true photoemission peak D, but the data of Garbe and Kirschner (1988) still clearly reveal it through an abnormal broadening of D. Returning briefly to the 19 eV spectra in figure 5, we can now understand the maximum observed at −2.5 eV, where the theoretical I_- spectrum has the minimum between C and B, as a secondary electron emission effect.

4. Conclusion

Comparison of calculated spin-resolved photoemission spectra with experimental data the same overall situation for the three cases Pd(111), Ir(111) and Pt(111). Theoretical peaks agree well with their experimental counterparts with regard to existence

and approximate position in energy. They can mostly be interpreted in terms of direct transitions from initial states of double-group symmetry Λ_{4+5}^3 and Λ_6^3 into Λ_6^1 states of the complex band structure. Deviations of up to about 0.3 eV between theory and experiment in initial state energies cannot be removed by reasonable changes in the final-state self-energy (i.e. in particular by shifting the 'upper band structure'), but rather reflect the usefulness as well as the limitations of approximating the real part of the quasi-hole self-energy by a ground state potential obtained self-consistently in a local density approximation.

Rather intriguing are the 'opposite-symmetry ghost peaks', which occur in the experimental spectra but are totally absent in the theoretical ones for emission angles up to $\pm 3°$ relative to the surface normal (corresponding to the acceptance cone in the available experiments). Some key to their explanation is provided by our finding that the intensity ratio between the leading peaks (labelled A and B in the above) in the experimental spectra comes closer to theory if one 'spin-flips' the ghost peaks back into the opposite-spin spectra. In search of their physical origin, one might first think of experimental reasons. If the measured spin polarisation is smaller than the one actually produced by circularly polarised light, e.g. because of incomplete circular polarisation of the radiation used, partial intensity spectra as obtained via equation (1) acquire ghost peaks. It appears that the observed ghosts are partly due to the 90% light polarisation, but a significant remainder might call for a physical mechanism, which is not included in our theory. Obviously, this phenomenon is observable only in spin-resolved but not in spin-averaged photoemission experiments.

The heights of the peaks from the lower Λ^3 pair (C and D) relative to the heights of those from the upper pair (A and B) are reasonably reproduced by the theory at most photon energies and indicate some preference of a linear over a quadratic form assumed for the inverse hole-lifetime. At photon energies, however, for which final state energies lie in a flat f-like band, experiment shows a strong enhancement of the intensity, which is not accounted for by our calculations, although a milder enhancement is produced in some cases. One might think of attributing at least part of the observed enhancement to the secondary-emission-type peak (discussed above in conjunction with figure 7), but further theoretical investigation seems needed.

Acknowledgments

This work was funded by the German Federal Ministry for Research and Technology under Contract No 05336CAB9. We would like to thank U Heinzmann and B Schmiedeskamp for useful discussions and for making available to us their Pd(111) data (Schmiedeskamp *et al* 1988) prior to publication. Likewise, we thank J Kirschner for making available new Pt(111) data (Garbe and Kirschner 1988) and discussing them with us. Our gratitude extends to N E Christensen for supplying us with his recent self-consistent potentials. Also, we are pleased to acknowledge the cooperative hospitality of the Institut für Festkörperforschung of the KFA Jülich.

References

Ackermann B and Feder R 1985a *J. Phys. C: Solid State Phys.* **18** 1093
—— 1985b *Solid State Commun.* **54** 1077

Baribeau J M, Carette J D, Jennings P J and Jones R O 1985 *Phys. Rev.* B **32** 6131
Barth U and Hedin L 1972 *J. Phys. C: Solid State Phys.* **5** 1629
Braun J, Thörner G and Borstel G 1985 *Phys. Stat. Solidi* (b) **130** 643
Christensen N E 1987 private communication
Eberhardt W and Plummer E W 1980, *Phys. Rev.* B **21** 3245
Eyers A, Schäfers F, Schönhense G, Heinzmann U, Oepen H P, Hünlich K, Kirschner J and Borstel G 1984 *Phys. Rev. Lett.* **52** 1559
Eyers A, 1984 *Dissertation,* Universität Bielefeld
Eyers A, Schönhense G, Friess U, Schäfers F and Heinzmann U 1985 *Surface Sci,* **162** 96
Feder R (ed.) 1985 *Polarised Electrons in Surface Physics* (Singapore: World Scientific)
Garbe J and Kirschner J 1988 to be published
Feibelman P J and Eastman D E 1974 *Phys. Rev.* B **10** 4932
Ginatempo B, Durham P J, Gyorffy B L and Temmerman W M 1985 *Phys. Rev. Lett.* **54** 187
Hedin L and Lundquist BI 1971 *J. Phys. C: Solid State Phys.* **4** 28
Heinzmann U 1987 *Physica Scripta T* **17** 77
Hora R and Scheffler M 1984 *Phys. Rev.* B **29** 692
Kirschner J 1985 *Polarised Electrons at Surfaces* (Heidelberg: Springer)
Noffke J and Fritsche L 1982 *J. Phys. F. Met. Phys.* **12** 921
McRae E G and Caldwell C W 1976 *Surf. Sci.* **57** 77
Müller N, Kessler B, Schmiedeskamp B, Schönhense G and Heinzmann U 1987 *Sol. State Commun.* **61** 187
Oepen H P, Hünlich K, Kirschner J, Eyers A, Schäfers F, Schönhense G and Heinzmann U 1985 *Phys. Rev.* B **31** 6846
Schmiedeskamp B, Kessler B, Müller N, Schönhense G and Heinzmann U 1988 *Solid State Commun.* **65** 665
Schmiedeskamp B, Vogt B and Heinzmann U 1988 *Phys. Rev. Lett.* **60** 651
Schönhense G 1986 *Appl. Phys.* A **41** 39
Speier W *et al* 1985 *Phys. Rev.* B **32** 359J
Tamura E, Feder R, Krewer J, Kirby R E, Kisker E, Garwin E L and King F K 1985 *Solid State Commun.* **5** 543
Tamura E and Feder R 1986 *Phys. Rev. Lett.* **57** 759
Tamura E, Piepke W and Feder R 1987 *Phys. Rev. Lett.* **59** 934
Treglia G, Ducastelle F and Spanjaard D 1982 *J. Phys.* **43** 341
Veen J F, Himpsel F J and Eastman D E 1980 *Phys. Rev.* B **22** 4226
Wern H, Courths R, Leschik G and Hüfner S 1985 *Z. Physik* B **60** 293
Wöhlecke M and Borstel G 1984 *Optical Orientation* ed. F Meier F and B P Zakharchenya (Amsterdam: North Holland)